

Optical identification of X-ray ROSAT sources in the field HS47.5/22

Dodonov S.N., Kotov S.S.

Institute of Applied Astronomy RAS,
Special Astrophysical Observatory RAS



Large Schmidt Telescopes of the World Ranked by full working aperture.

d / D / F	Tel. Name	Institution	Location
134/200/400	Karl-Schw. Obs.	TLS	Tautenburg, Germany
125/183/307	Oschin Schm.	Mt. Palomar Obs.	Calif., USA
124/187/307	UK Schm. Tel.	UK Schmidt	Anglo-Aus Obs., Australia
105/150/325		Kiso Obs.	Japan
102/132/213		Byurakan Obs.	Armenia
100/135/300		Kvistaberg Observatory	Uppsala, Sweeden
100/160/306		ESO	Chile
100/152/300		Llano del Hato Obs.	Venezuela
66 /66 /91	The New C.S.S. Schmidt	Steward Obs./LPL/U.of Az	Arizona, USA
61 /91 /208	Burrell Schm.	Warner & Swasey Obs/CWRU	Kitt Peak, USA
61 /91 /208	Curtis Schm.	U. of Mich.CTIO,	Chile
60 /91 /184		Southern Uppsala Sch.	Siding Spr. Obs., Aus
60 /91 /184		Campo Imperatore Obs.	Gran Sasso Mtn., Italy
50 /75 /150	Brorfelde Schm.	Brorfelde Obs.	Copenhagen, Denmark
67 /92 / ?	Large Schmidt	Asiago Obs.	Universita di Padova, Italy
53 /53 /160		Byurakan Obs.	Armenia
40 /50 / ?	Smaller Schmidt	Asiago Obs.	Universita di Padova, Italy
42 /66 /91	The Old C.S.S.Schmidt	Steward Obs./LPL/U.of Az	Arizona, USA

Instrumentation : 1-m Schmidt Telescope + Apogee Alta U16M.



Telescope mirror :

Diameter 1320 mm
Focal Length 2130 mm
Image Scale 96.7 "/mm
Field of View ~16 sq. deg.

Corrector Lens

1020 mm

Objective Prisms :

Diameter 1000 mm
1.5 deg 1800 A/mm
3.0 deg 900 A/mm
4.0 deg 280 A/mm

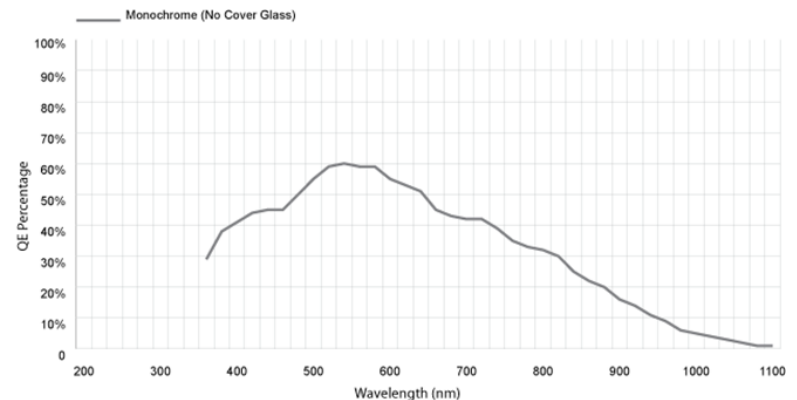
Detector :

Kodak KAF-16803 4k x 4k
Pixel Size 9 μ k x 9 μ k
Readout Noise <11 e
Dark Current < 0.01 e/sec
Q.E. 35 % (3500 A)
60 % (5500 A)
18 % (9000 A)

Field of View ~ 1 sq. deg

Image Scale 0.868 arcsec/pix

Liquid Cooling $\pm 0.1^\circ\text{C}$



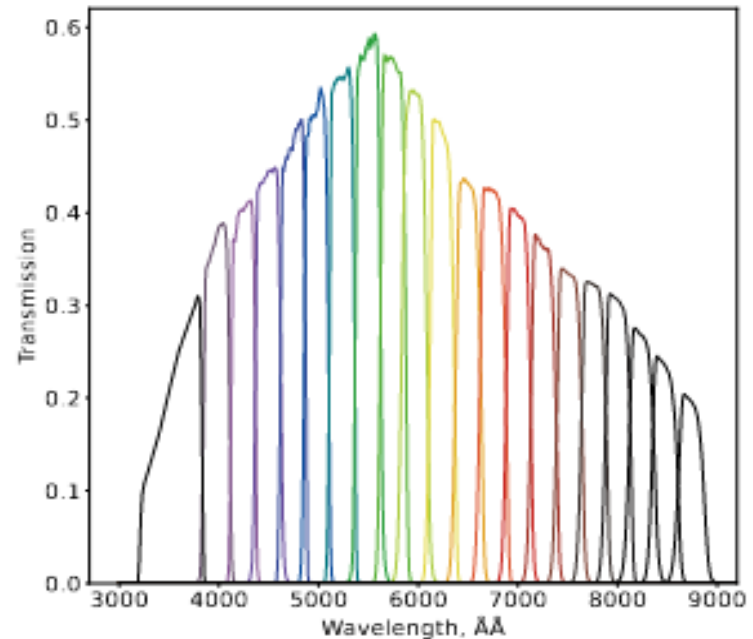
Observations on 1-m Schmidt Telescope.



Telescope field of view with 4k x 4k CCD 58 x 58 arcmin, scale 0.868 arcsec/pixel.

Observations were in four broad band filters (u, g, r and i SDSS) and in 16 medium band (FWHM=250 Å) filters. Total exposure time in filters were varied from 60 min to 120 min depending from the spectral sensitivity of the CCD.

Filter	lambda_cen, Å	FWHM (Å)	m_lim,3 sigma
u_SDSS	3578	338	24.23
g_SDSS	4797	860	25.22
r_SDSS	6227	770	24.97
i_SDSS	7624	857	24.15
MB_400	3978	250	24.37
MB_425	4246	250	24.31
MB_450	4492	250	24.20
MB_475	4745	250	24.31
MB_500	4978	250	24.30
MB_525	5234	250	24.37
MB_550	5496	250	23.86
MB_575	5746	250	24.29
MB_600	5959	250	23.89
MB_625	6234	250	23.51
MB_650	6499	250	23.41
MB_675	6745	250	23.78
MB_700	7002	250	23.47
MB_725	7253	250	23.20
MB_750	7519	250	23.07
MB_775	7758	250	22.97



Medium band filters set used in observations.
CCD spectral response included.

Observations on 1-m Schmidt Telescope.



HS47.5-22

RA = $09^{\text{h}}50^{\text{m}}00^{\text{s}}$ DEC = $+47^{\text{d}}35^{\text{m}}00^{\text{s}}$

Mosaic of 4 x 1 sq. deg. fields with
10 arcmin overlap.

Final field size **2.38** sq. deg.

16 Medium Band Filters with
FWHM = 250 Å.

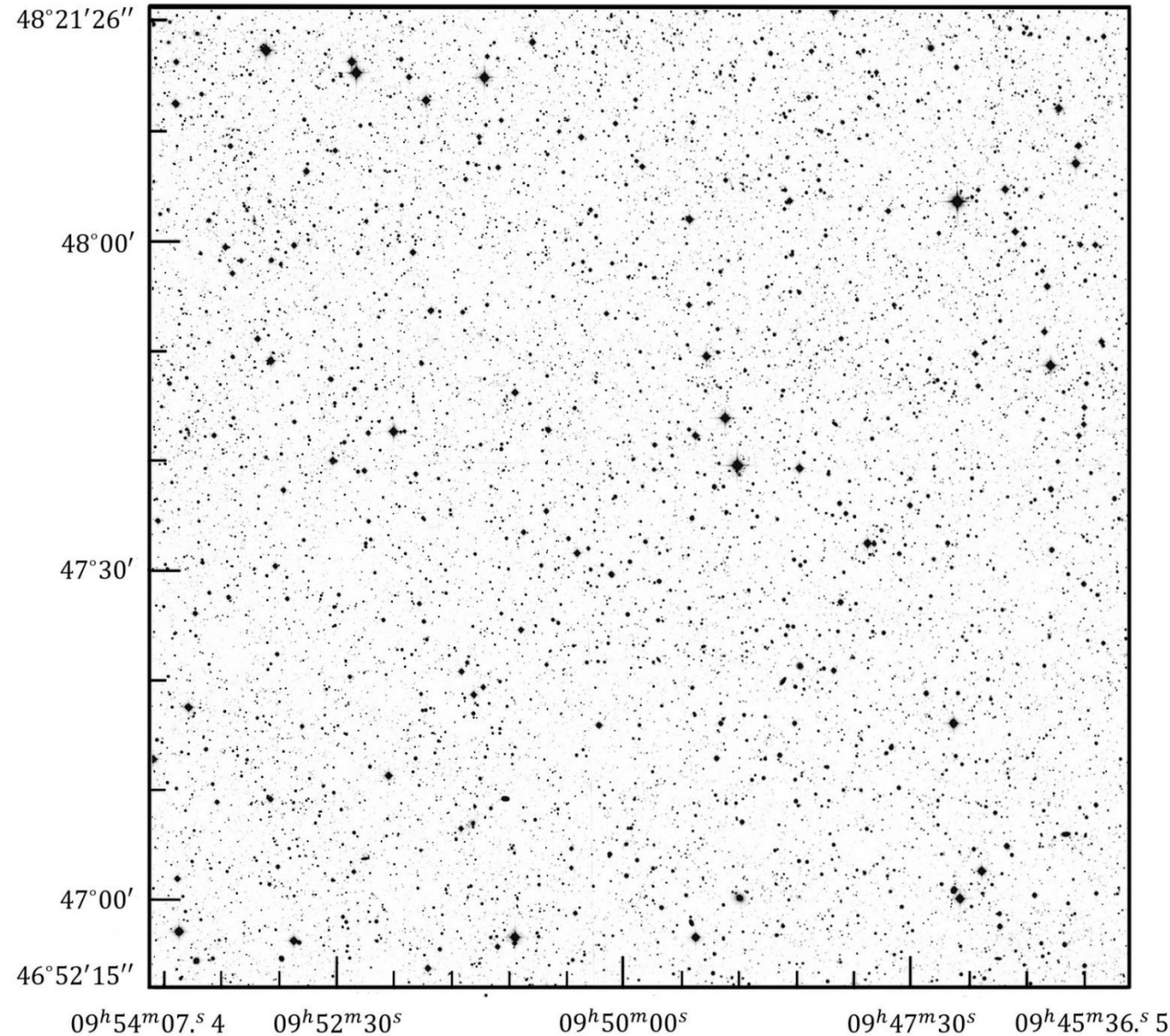
4 Broad Band SDSS Filters.

Homogeneous spectral coverage
4000 - 8000 Å with S/N $\sim 3 - 5$ at
AB=23^m in all medium band filters.

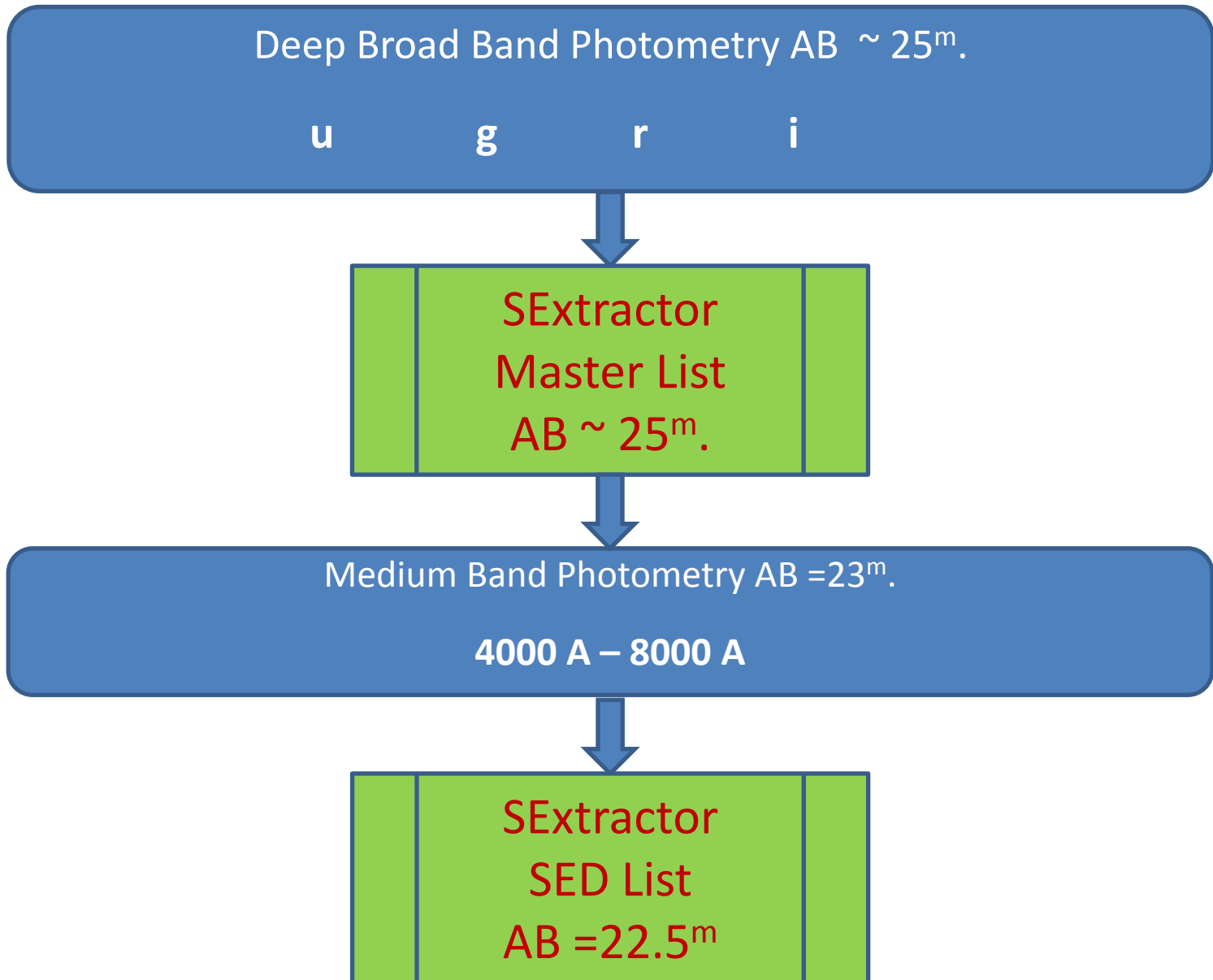
144 ROSAT Objects
to 3.5×10^{-14} ergs $\text{cm}^{-2}\text{s}^{-1}$

362 FIRST Objects

236 SDSS QSO



Data Reduction Flow.



Photometric data catalog of the HS47.5/22 field.



The selection of objects of the HS47.5/22 field is based on the sum of deep ($m_{AB} \sim 25^m$) images in broadband filters (g_SDSS + r_SDSS + i_SDSS). Photometry of objects was performed using an SExtractor (Bertin & Arnouts 1996) in the fashion of double images. The sum of the deep ($\sim 25^m$) images obtained in the g, r, i SDSS filters was used as the reference image from which the coordinates of the objects were determined. The resulting catalogs of objects were combined into a common catalog using astrometric coordinates.

The total number of objects in the HS47.5/22 field up to $r_{AB} \approx 24^m.5$ is 85332.

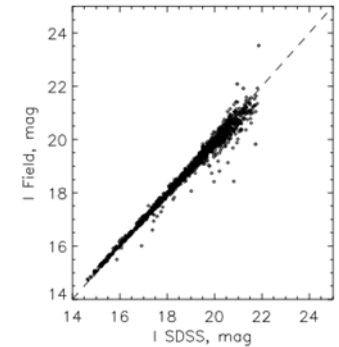
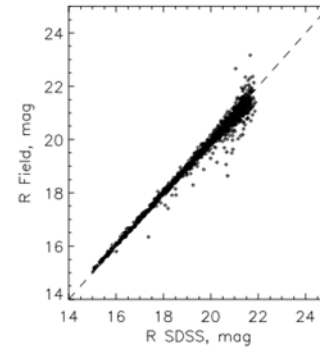
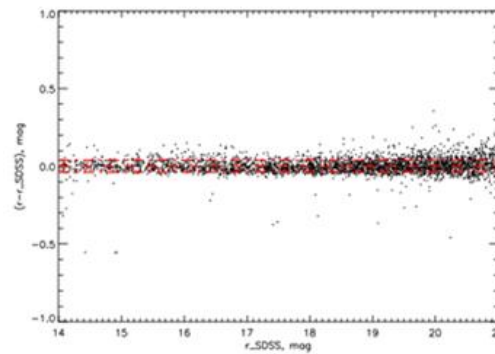
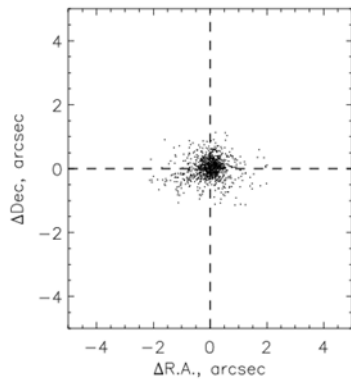
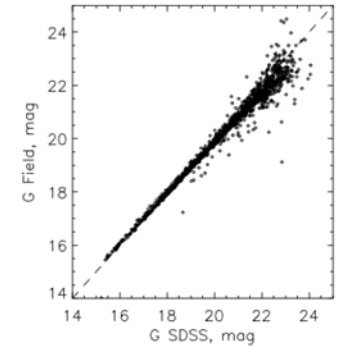
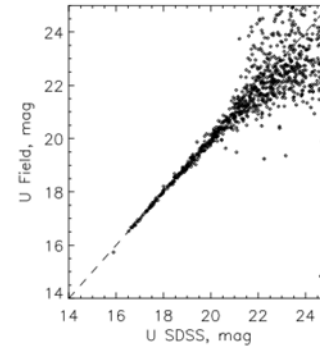
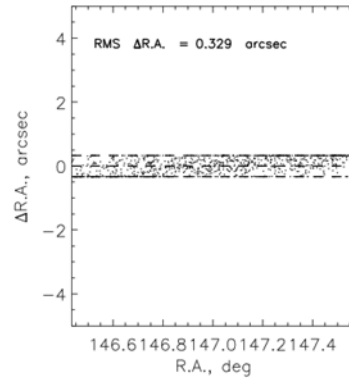
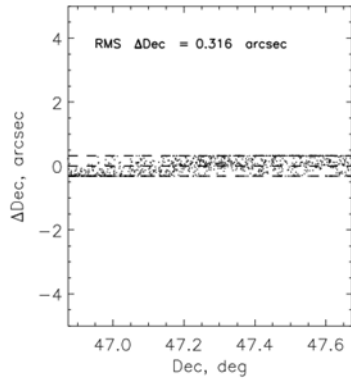
The complete sample of the field objects (28564 objects) is limited by the limiting stellar magnitude $r_{AB} \approx 22.5^m$, up to which images were obtained in medium-band filters has a signal-to-noise ratio of 5-10.

The combined catalog of objects is supplemented by WISE infrared photometry data (Meissner et al., 2018), broadband photometry and spectral SDSS data (Paris et al., 2018), DECaLS photometry (Day et al., 2019), morphology data from the DECaLS survey and data on proper movements of the objects from the GAIA survey (Gaia Collaboration et al., 2018).

Using the morphological classification of the DECaLS survey (image quality in images of the order of 1 arcsec), we divided the combined catalog of objects of the HS47.5/22 field into two subsamples: extended (galaxies) and star-like objects. The analysis of the samples was carried out separately, the details of the analysis are published in (Grokhovskaya et al., 2022) and (Kotov et al., 2022).



Astrometry and Photometry.



Schmidt Astrometry vs SDSS Astrometry.

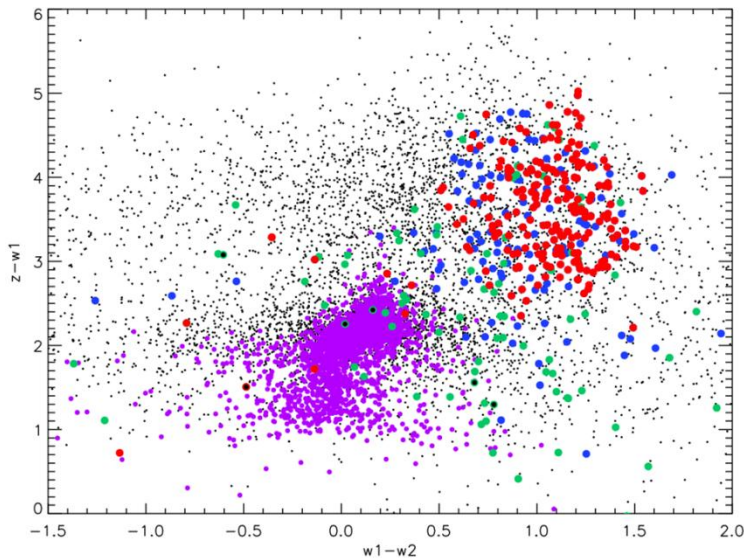
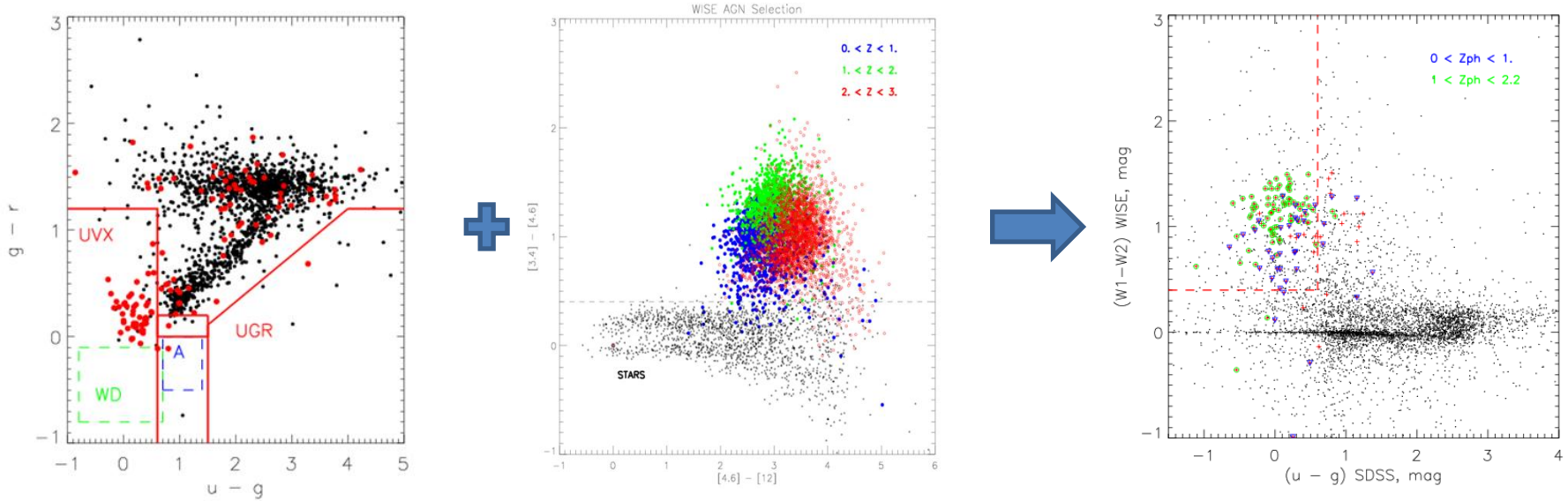
RMS = 0.38

Schmidt Photometry vs SDSS Photometry.

$(u - u_{SDSS}) \Rightarrow \sigma = 0^m.11$ $(g - g_{SDSS}) \Rightarrow \sigma = 0^m.05$

$(r - r_{SDSS}) \Rightarrow \sigma = 0^m.04$ $(i - i_{SDSS}) \Rightarrow \sigma = 0^m.04$

QSO selection.

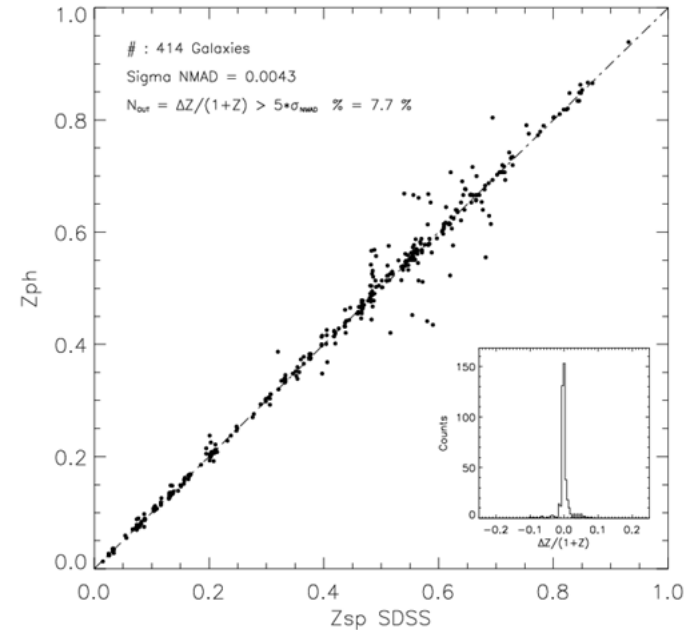
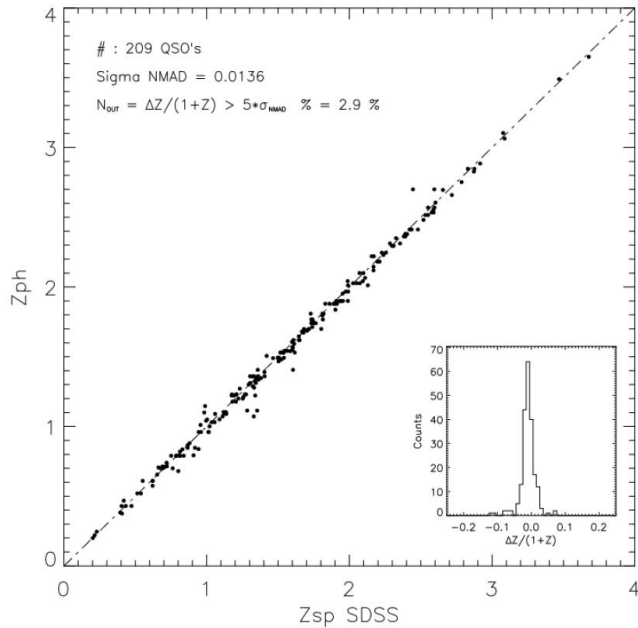


The completeness of the QSO selection according to the diagram $(u - g) - (W1-W2)$ for objects with $0 < Z < 1$ is 73%, and for objects with $1 < Z < 2.2$ is 92% for $r_{SDSS} = 22.5^m$

In the left diagram $(z - W1) - (W1 - W2)$, spectrally confirmed quasars are indicated in red, candidates for quasars are indicated in blue, stars (objects with proper motions $> 3\sigma$ according to GAIA data) are indicated in purple, (Kotov et al., 2022).



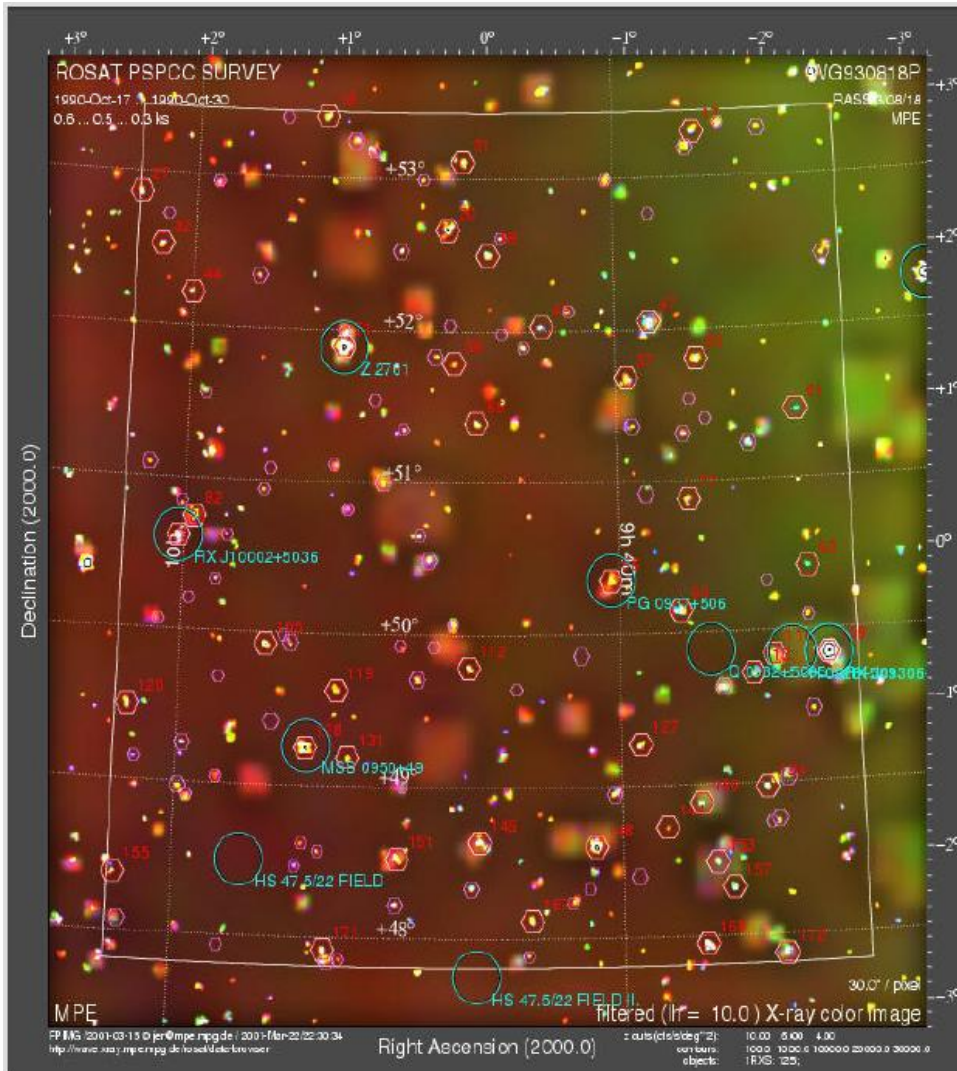
Photometric redshifts.



Photometric redshifts were obtained using the ZEBRA software (Feldman et al., 2009) and a set of synthetic LePHare templates. A total of 682 QSO candidates with photometric redshifts from $Z_{ph} = 0.1$ to $Z_{ph} = 5.2$ were identified, (Kotov et al., 2022).

A complete sample of galaxies up to $r=22^m.5$: 19126 objects. Analysis of the large-scale distribution of galaxies using sophisticated OPTICS algorithms (Ankerst et al., 1999); We found 534 groups of the galaxies with a number of members above 3 to $Z_{ph} = 0.8$, (Grokhovskaya et al., 2022).

ROSAT PSPCC SURVEY : FIELD HS47.5/22



The choice of the field for observations is due to its location in an area with a very low density of neutral hydrogen on the line of sight $\langle N_{\text{H}} \rangle = 10^{20} \text{ cm}^{-2}$, which is not much higher than the absorption value in Lockman Hole, where the lowest absorption on the line of sight for the northern sky is observed $\langle N_{\text{H}} \rangle = 4.5 \times 10^{19} \text{ cm}^{-2}$.

ROSAT observations consist of a series of overlapping PSPCC regions and were conducted between April 1991 and October 1993. The total exposure time is > 5000 seconds for 73% of the area and more than 20000 seconds for the central area with a size of 2.3 sq. deg. The limiting flux of $3.4 \times 10^{-14} \text{ ergs cm}^{-2} \text{ s}^{-1}$ was obtained for objects in the range 0.1-2.4 keV.

HS 47.5/22 (09^h50^m00^s +47°50'00", 2000)



Optical identification.

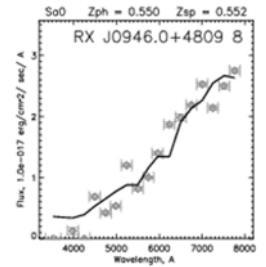
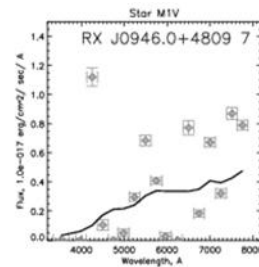
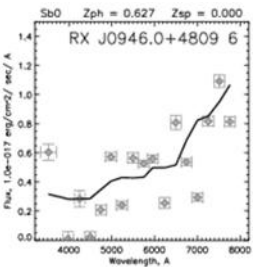
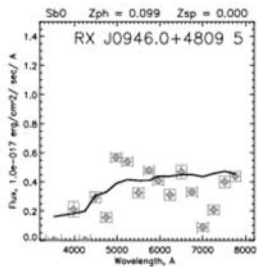
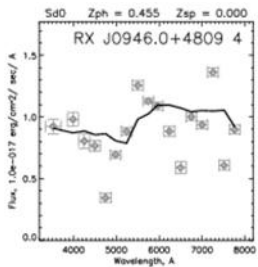
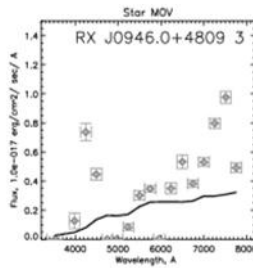
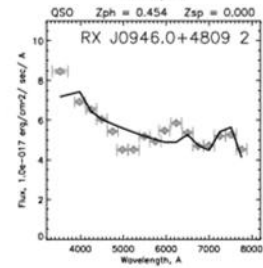
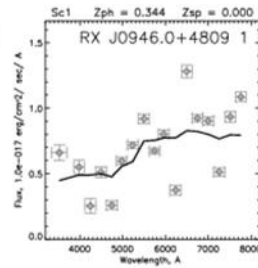
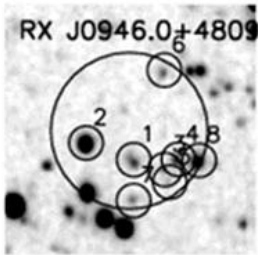
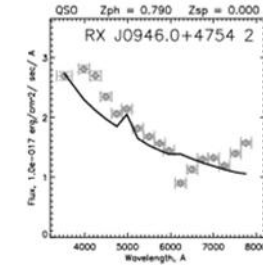
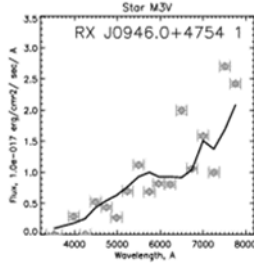
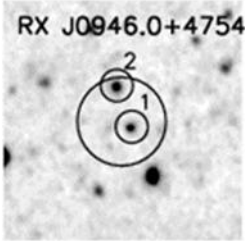
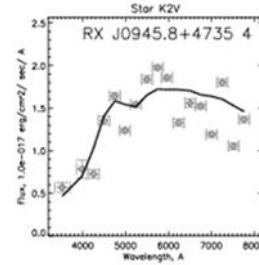
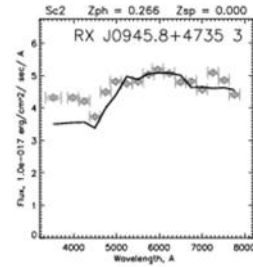
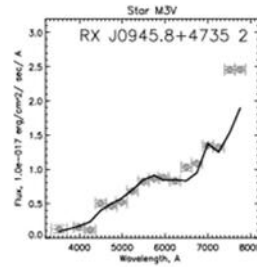
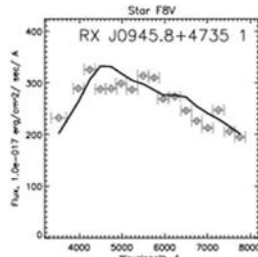
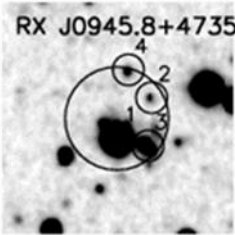
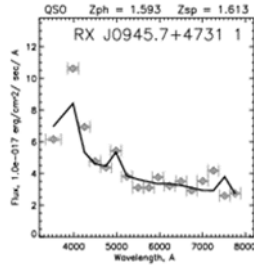
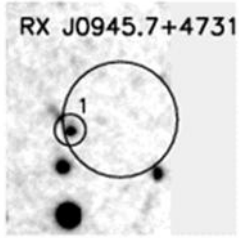
For optical identification, data from the Molthagen, Wendker, & Briel, 1997 catalog were taken, which included 574 X-ray sources and data from our combined catalog. As a **box of errors** in the position of X-ray sources, we chose a radius of **$3\sigma+10''$** . The choice of the size of the error box was made taking into account the systematic positional shifts found during the creation of the RX2 catalog (Boller et al., 2016).

For our optical data there are two values determining the identification of X-ray objects : the **limiting magnitude of object detection** : $r_{AB}=24^m.97$, and the **limiting magnitude of classification and determination of photometric redshifts of objects** based on their energy distributions constructed in medium-band filters : $r_{AB}=22^m.5$, depending on the type of object spectrum. Thus, if objects are not detected in the error box ("empty field") we can state that the possible sources of X-ray radiation are fainter than $r_{AB}\sim 25^m$.

The identification procedure found 5 "empty fields" and 449 objects that fell into the coordinate error boxes of X-ray sources. Among them are 85 QSOs, 126 stars of different spectral classes and 238 galaxies. In addition, 4 radio sources from the FIRST catalog were found.



Optical identification.

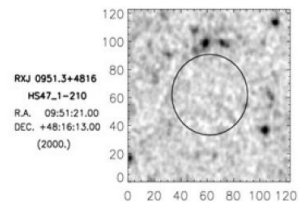


Optical identification, results.

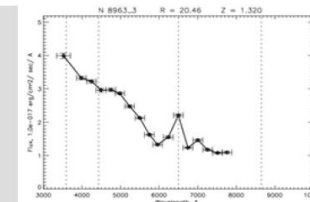
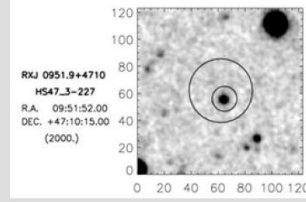


Rosat ID	Counts	Box	N	R.A. (J2000.0)	Dec.(J2000.0)	Δr	m_r	Z_{ph}	Z_M	Z_{SDSS}	Type	Comments	
RX J0945.7+4731	6.2	29	1	09 45 49.67	+47 31 16.26	27.0	19.91	1.593	1.613	QSO		
RX J0945.8+4735	7.5	26	1	09 45 49.10	+47 35 03.70	11.1	15.10	Star F8V		
			2	09 45 47.37	+47 35 24.59	19.6	21.16	Star M3V		
			3	09 45 47.58	+47 34 59.84	21.1	19.39	0.266	Sc2	
			4	09 45 48.54	+47 35 38.94	24.8	20.63	Star K2V	
RX J0945.8+4654	3.7	22	1	09 45 50.56	+46 54 06.68	8.6	21.04	Star K7V		
			2	09 45 51.94	+46 53 53.26	11.1	20.70	Star M2V	
			3	09 45 52.62	+46 54 01.34	16.0	19.89	Star K4V	
			4	09 45 50.32	+46 54 17.72	19.5	20.73	Star K0V	
RX J0945.9+4748	4.1	23	1	09 45 51.89	+47 48 00.31	14.5	14.66	Star K0V		
			2	09 45 53.84	+47 48 21.68	19.3	17.10	Star K2V	
RX J0946.0+4754	2.1	22	1	09 46 00.63	+47 54 22.73	5.3	21.08	Star M3V		
			2	09 46 01.35	+47 54 43.29	17.8	20.78	0.790	QSO	
RX J0946.0+4809	7.5	37	1	09 46 03.87	+48 09 33.66	14.2	21.32	0.344	Sc1	
			2	09 46 06.11	+48 09 41.74	21.4	19.33	0.454	QSO	
			3	09 46 02.40	+48 09 28.89	25.1	21.98	Star M0V	
			4	09 46 01.76	+48 09 33.75	26.9	21.05	0.455	Sd0	
			5	09 46 02.18	+48 09 22.98	31.1	22.22	0.099	Sb0	
			6	09 46 02.40	+48 10 15.99	32.7	21.46	0.627	Sb0	
			7	09 46 03.89	+48 09 14.32	33.4	22.13	Star M1V	
			8	09 46 00.78	+48 09 33.20	35.8	20.47	0.550	0.552	Sa0	
RX J0946.0+4735	5.8	20	1	09 46 04.44	+47 35 10.54	5.5	19.16	0.144	QSO	FIRST J094604.5+473510.1
			2	09 46 02.57	+47 35 13.39	16.4	21.68	Star F2V	
			3	09 46 02.47	+47 34 58.88	17.9	20.20	Star M2V	
RX J0946.2+4745	1.8	23	1	09 46 11.00	+47 45 31.13	11.6	20.52	2.516	2.549	QSO	
			2	09 46 14.13	+47 45 37.07	21.0	22.25	0.467	Sdm	
			3	09 46 14.26	+47 45 42.56	23.2	22.33	1.057	Sb1	
RX J0946.3+4804	3.6	34	1	09 46 17.51	+48 04 32.72	9.6	20.33	1.506	1.420	QSO	
			2	09 46 17.11	+48 04 40.62	18.5	21.86	1.410	QSO	
			3	09 46 18.04	+48 03 56.85	27.8	20.72	0.112	Sc0	
			4	09 46 16.01	+48 04 01.04	31.3	20.71	0.406	Sc0	
RX J0946.3+4711	130	13.0	0									Empty Field	
RX J0946.3+4752	4.2	23	1	09 46 23.49	+47 53 01.75	10.9	19.04	1.050	1.003	QSO	
			2	09 46 22.26	+47 53 14.04	23.7	20.72	0.589	Sc0	

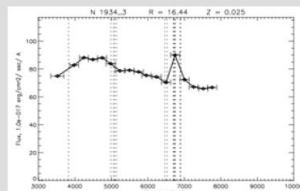
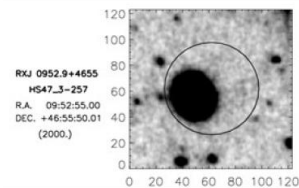
Optical identification, examples.



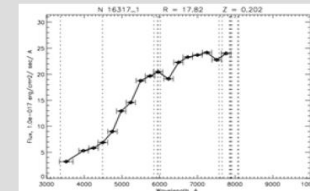
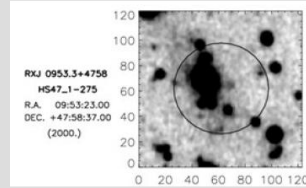
Пустое поле (объектов ярче $R_{AB}=24.97$ не обнаружено)



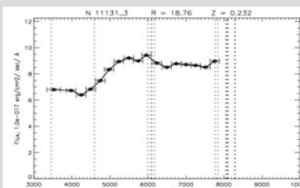
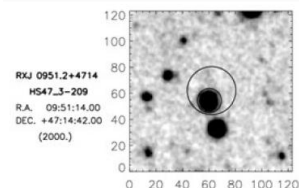
Квazar $Z=1.320$



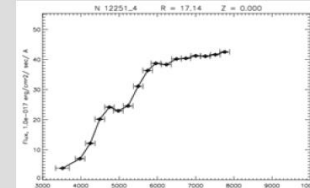
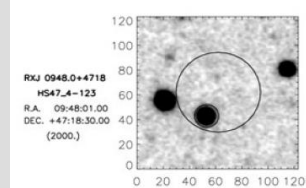
Яркая галактика
 $Z=0.025$



Скопление галактик
 $Z=0.202$

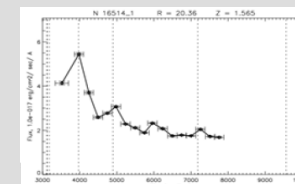
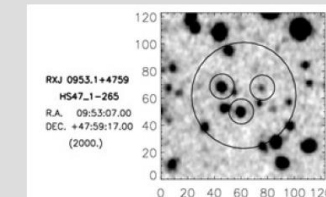


Галактика с эмиссией
 $Z=0.025$

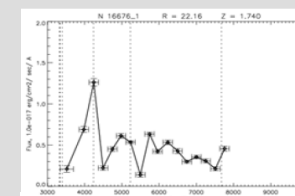


Звезда

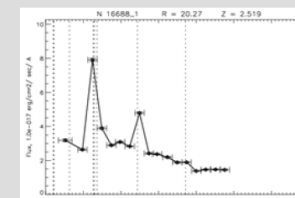
We found 5 "empty fields" and 449 objects that fell into the coordinate error boxes of X-ray sources. Among them are **85 QSOs**, **126 stars** of different spectral classes and **238 galaxies**. In addition, 4 radio sources from the FIRST catalog were found.



Квazar $Z=1.565$



Квazar $Z=1.740$



Квazar $Z=2.519$